

# Paclitaxel

Subjects: **Others**

Contributor: Paula Montero

Paclitaxel is an anticancer drug, extracted from the bark of the Pacific yew tree *Taxus brevifolia*. It was first approved in 1992 by the US Food and Drug Administration (FDA) for the treatment of advanced ovarian cancer and since then, it has been used in several cancers such as breast cancer, endometrial cancer, non-small-cell lung cancer, bladder cancer, cervical carcinoma, and AIDS-related Kaposi sarcoma.

paclitaxel

epidermis

NHEK

## 1. Non-Cytotoxic Doses of Paclitaxel Induce Inflammation in a 3D Epidermis Model

The effects of paclitaxel on cell viability were examined in NHEK cells. Incubation with the positive control SLS demonstrated that both assays were sensitive to changes in viability and cytotoxicity. Treatment with increasing doses of paclitaxel (0.3–30  $\mu\text{M}$ ) for 24 h was safe for NHEK keratinocytes as it did not induce significant viability reduction and LDH release. The mean viability percentages were  $86.53 \pm 3.5\%$ ,  $94.46 \pm 0.8\%$ , and  $97.35 \pm 1.085\%$  at concentrations 30  $\mu\text{M}$ , 3  $\mu\text{M}$ , and 0.3  $\mu\text{M}$ , respectively (**Figure 1A**). The LDH release was lower than 2.5% in all doses examined and was not significant compared to the control (**Figure 1B**). The stratification of the 3D epidermis cell model was confirmed by the hematoxylin-eosin staining as shown in **Figure 2A**. Keratinocytes were distributed into the principal epidermis layers. The basal, spinous, and granular layers are present in the reconstructed model and its terminal differentiation resulted in the presence of the stratum corneum, analogously to the epidermal *in vivo* structure of healthy skin. Since IL-1 $\alpha$ , IL-6, and IL-8 are known as skin inflammation molecular markers [1][2][3], and these markers have been found to be upregulated by paclitaxel in some cancer cell lines [4][5][6], we analyzed whether paclitaxel could mediate an inflammatory response in the 3D epidermis model through the induction of such cytokines. Incubation of the 3D model with paclitaxel induced a significant dose-dependent release of IL-1 $\alpha$ , IL-6, and IL-8 (**Figure 2B–D**).

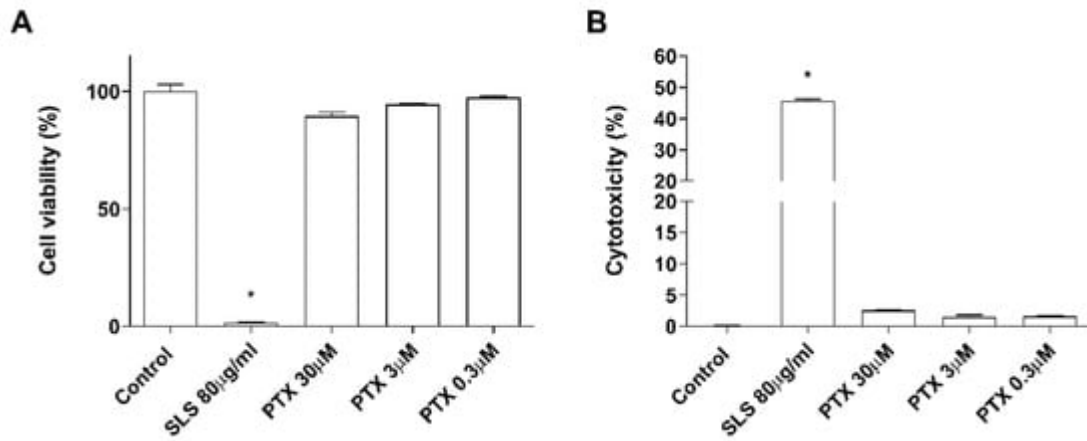


**Figure 1.** Paclitaxel does not modify cell viability and cytotoxicity. NHEK cells were incubated for 24 h with increasing paclitaxel concentrations. (A) Paclitaxel, at the concentrations assayed did not show alterations on cell viability measured by the MTT assay (B) nor in the cytotoxicity measured by LDH assay. Results are expressed as mean  $\pm$  standard deviation of three independent experiments ( $n = 3$ ). Multiple comparisons analysis of variance (ANOVA) was followed by the post hoc Bonferroni test. \*  $p < 0.05$  vs. control. PTX: paclitaxel. SLS: sodium lauryl sulfate.

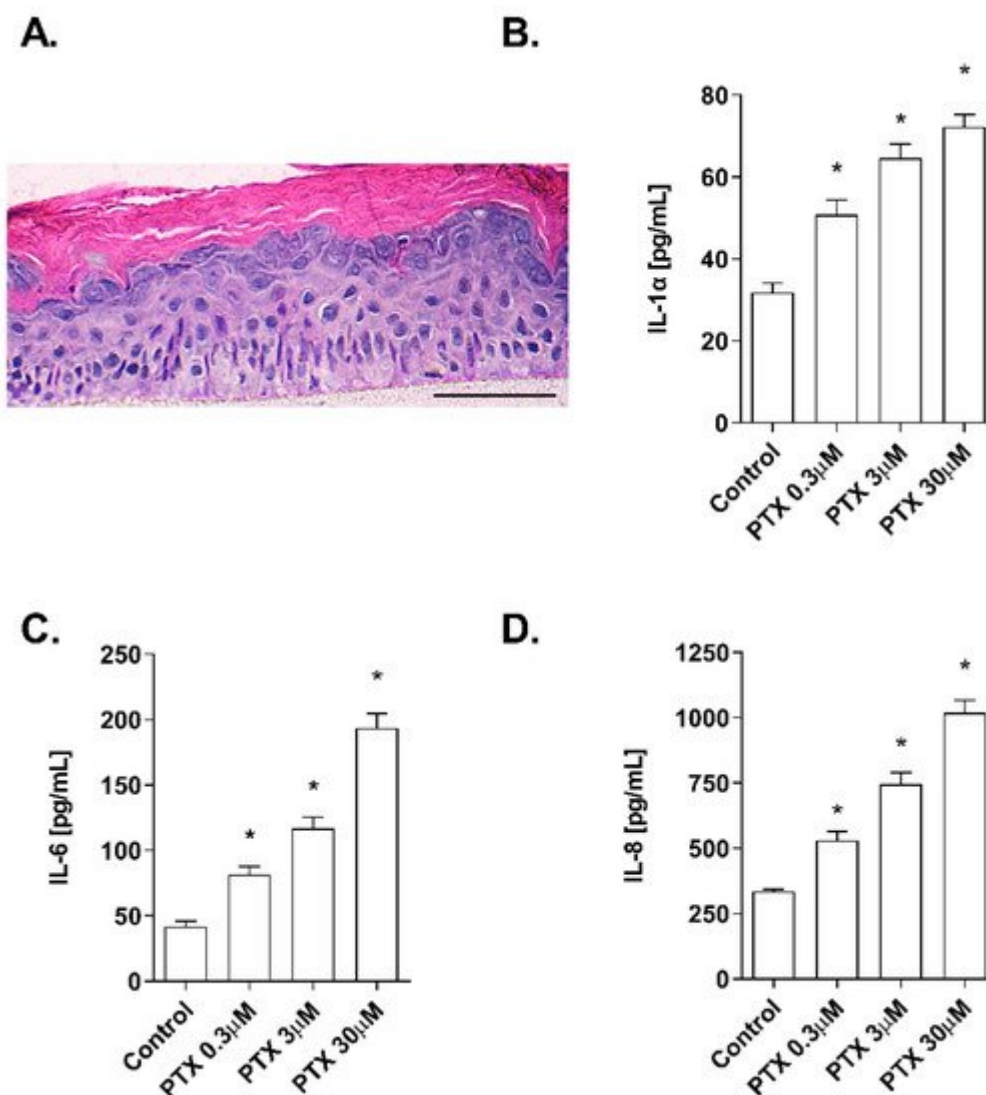


**Figure 2.** Paclitaxel induces a dose-dependent inflammatory cytokine release in a 3D epidermal model. (A) Paraffin section from the 3D epidermis model stained with hematoxylin and eosin. Scale bar 100  $\mu$ M. The 3D epidermal model was incubated for 24 h with increasing paclitaxel concentrations. (B) IL-1 $\alpha$ , (C) IL-6, and (D) IL-8 levels were measured by ELISA. Results are expressed as mean  $\pm$  standard deviation of three independent experiments ( $n = 3$ ). Multiple comparisons analysis of variance (ANOVA) was followed by the post hoc Bonferroni test. \*  $p < 0.05$  vs. control. PTX: paclitaxel.

## 2. Paclitaxel-Induced Oxidative Stress Response

As it has been proposed that the apoptotic effects of paclitaxel may be mediated by its capacity to induce the release of reactive oxygen species (ROS) [7][8][9], the effect of paclitaxel on intracellular ROS levels was analyzed in NHEK cells and in a 3D epidermis model. As shown in **Figure 3A**, exposure to paclitaxel doses of 0.3, 3, and 30  $\mu$ M for 4 h, caused a significant increase in ROS production. To assess which molecules might be taking part in the oxidant induction of paclitaxel, gene, and protein expression of nuclear factor erythroid-2-related factor 2 (Nrf2), superoxide dismutase (SOD1), and NADPH oxidase 4 (NOX4) were analyzed in the 3D epidermal model. Nrf2 is a

transcription factor that regulates the endogenous antioxidant defense, SOD1 is a ROS scavenging gene and NOX4 is one of the primary enzymatic sources of ROS. Treatment of this model with paclitaxel for 24 h induced a decrease in the mRNA expression of SOD1 and Nrf2 in a dose-dependent manner (**Figure 3B**). The same incubation time induced the upregulation of NOX4 in all paclitaxel doses (**Figure 3B**). **Figure 3C** shows that incubating the 3D epidermis model for 24 h with paclitaxel produced the same response in the protein expression as in the mRNA expression: A concentration-dependent decrease in both SOD1 and Nrf2 protein expression and a concentration-dependent increase in NOX4.

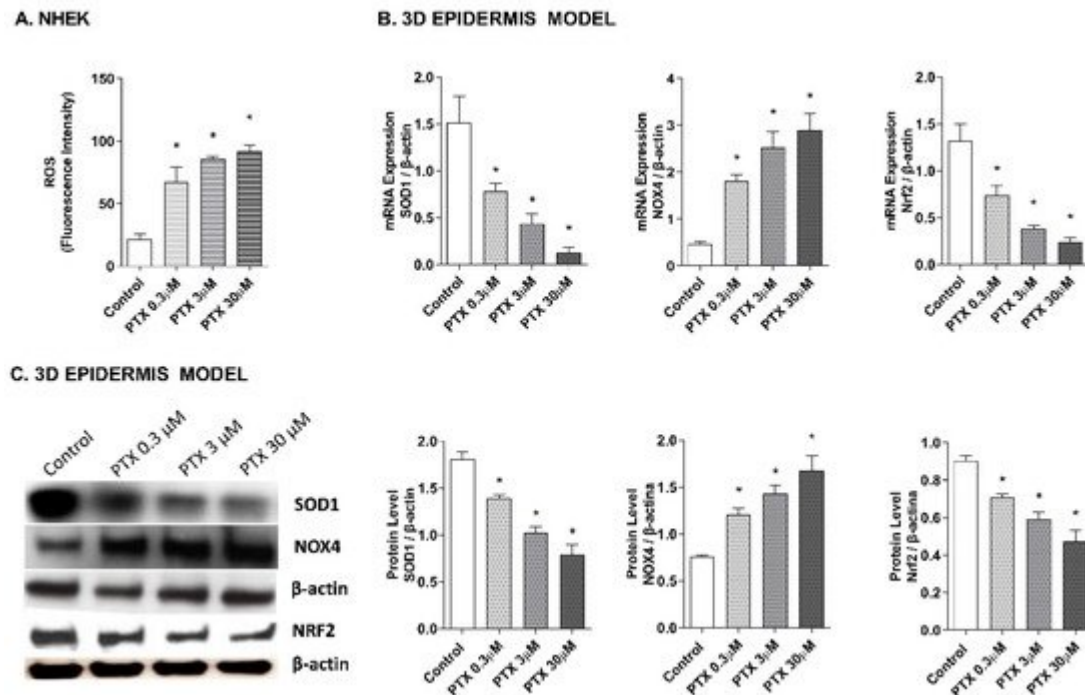


**Figure 3.** Paclitaxel induces a dose-dependent oxidative stress response in normal human epidermal keratinocytes (NHEK) cells and in a 3D epidermal model. (A) NHEK cells were incubated for 4 h with increasing paclitaxel concentrations. Quantification of reactive oxygen species (ROS) levels measured by the H<sub>2</sub>DCF-DA assay. Data are expressed as reactive oxygen species (ROS) DCF relative fluorescence units. (B) 3D epidermal model tissues were incubated for 24 h with increasing paclitaxel concentrations. SOD1, Nrf2 and NOX4 mRNA levels were measured by real-time PCR. Data are expressed as 2<sup>-ΔCt</sup>. (C) 3D epidermal model tissues were incubated for 24 h with increasing paclitaxel concentrations. SOD1, Nrf2 and NOX4 protein levels were analyzed by western blotting. Quantification was performed by densitometry and normalized to β-actin. Results are expressed as mean ± standard deviation of three independent experiments (n = 3). Multiple comparisons analysis of variance (ANOVA) was followed by the post hoc Bonferroni test. \* p < 0.05 vs. control. PTX: paclitaxel.

### 3. Paclitaxel-Induced Apoptosis

Detection of annexin V-FITC by flow cytometry was used to analyze the apoptosis percentage induced by paclitaxel in NHEK cells (**Figure 4A,B**). Keratinocytes incubation with paclitaxel for 24 h induced an increase in cellular apoptosis. Representative propidium iodide versus annexin V-FITC plots are shown in **Figure 4A** for each

condition. Higher doses of paclitaxel induced significantly higher apoptosis rates, reaching up to  $25.8 \pm 2.9\%$  apoptosis at the highest dose  $30 \mu\text{M}$  (**Figure 4B**). To analyze the apoptosis molecular markers in the 3D epidermis model, gene and protein expression of p53, p21, and BCL2 were measured (**Figure 4C–E**). 24 h of paclitaxel incubation reduced BCL2 mRNA expression while p53 and p21 were upregulated. All markers showed a dose-dependent modulation and statistically significant variations. Protein levels of BCL2 and p53 were also analyzed by Western blot and showed a dose-dependent increase in the case of p53, while protein levels of BCL2 decreased significantly (**Figure 4F**).

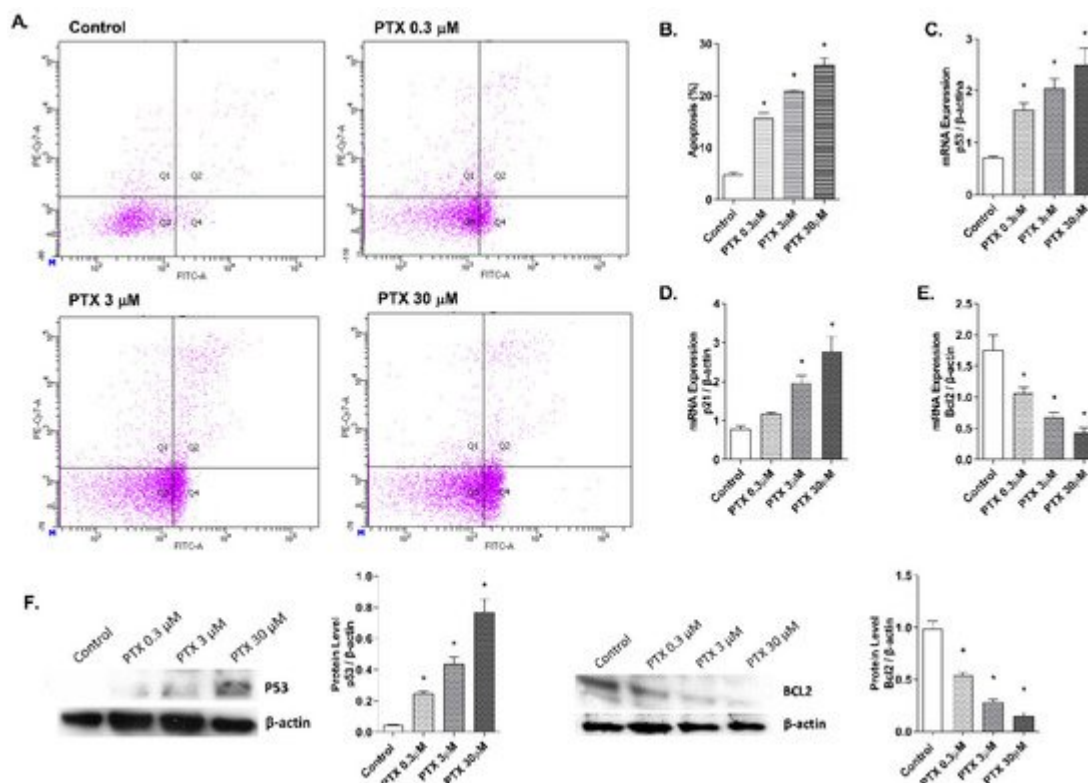


**Figure 4.** Paclitaxel induces apoptosis in normal human epidermal keratinocytes (NHEK) cells. (A) NHEK cells were incubated for 24 h with increasing paclitaxel concentrations. Apoptosis was measured by flow cytometric analysis. (A) Representative plots for each paclitaxel concentration are displayed. (B) Apoptosis plots were analyzed by FlowJo software (TreeStar Inc., Ashland, OR, USA). Results are expressed as the mean apoptosis percentage of annexin-positive and propidium iodide-negative cells, which represent early apoptotic cells. (C–E) 3D epidermal model tissues were incubated for 24 h with increasing paclitaxel concentrations. P53, p21, and BCL2 mRNA levels were measured by real-time PCR. Data are expressed as  $2^{-\Delta\text{Ct}}$ . (F) 3D epidermal model tissues were incubated for 24 h with increasing paclitaxel concentrations. P53 and BCL2 protein levels were analyzed by Western blotting. Quantification was performed by densitometry and normalized to  $\beta$ -actin. Results are expressed as mean  $\pm$  standard deviation of three independent experiments ( $n = 3$ ). Multiple comparisons analysis of variance (ANOVA) was followed by the post hoc Bonferroni test. \*  $p < 0.05$  vs. control. PTX: paclitaxel.

## 4. Paclitaxel-Targeted Angiogenesis

Paclitaxel has a strong anti-angiogenic activity in cancer cells through the suppression of the vascular endothelial growth factor (VEGF) expression, which plays a main role in the growth of new blood vessels, by activating the endothelial nitric oxide synthase (eNOS) [10][11][12]. To evaluate these events in the skin, the effect of paclitaxel on endothelial tube formation was examined in human dermal microvascular cells. Representative images for each condition are shown in **Figure 5A**. HDMECs in the control condition formed capillary-like structures. However, incubation with paclitaxel for 16 h showed an impairment of angiogenesis in all doses. The analysis was performed by measuring the significant decrease of the tube length, total branches and total loops created by HDMECs in the gel matrix after paclitaxel incubation (**Figure 5B**). The molecular markers of angiogenesis, VEGF and eNOS, were also evaluated in the 3D epidermis model. After paclitaxel treatment, VEGF and eNOS mRNA expression were significantly reduced in a dose-dependent manner (**Figure 5C**). The same decrease was induced by paclitaxel in VEGF protein levels (**Figure 5D**).

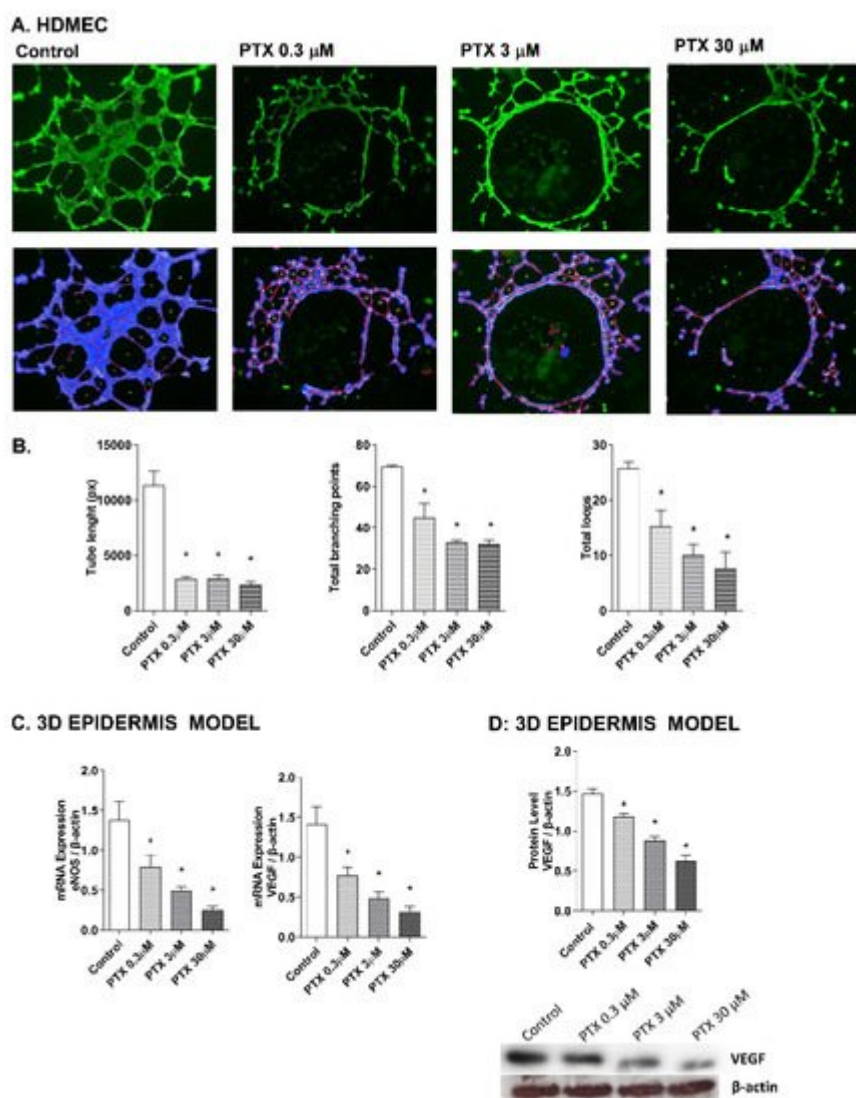


**Figure 5.** Paclitaxel inhibits endothelial tube formation in human dermal microvascular endothelial cells (HDMEC) and reduces eNOS and VEGF expression in the 3D epidermis. (A) HDMEC were incubated with increasing paclitaxel concentrations for 16 h, and angiogenesis was analyzed by the endothelial tube formation assay. Representative images of the tubular structures formed are displayed. Top images show the green, fluorescent

calcein staining. Bottom images show the overlay generated by WimTube™ software (Onimagin Technologies SCA, Córdoba, Spain), in which each color represents a structure: blue represents the covered area, red the tubes, white the branching points and yellow the number of loops. **(B)** Quantitative evaluation of morphological features of the capillary-like network structure. Tube length, total branching points and total loops after treating HDMEC with increasing paclitaxel concentrations. The analysis was performed using WimTube™ software (Onimagin Technologies SCA, Córdoba, Spain). **(C)** 3D epidermal model tissues were incubated for 24 h with increasing paclitaxel concentrations. eNOS and VEGF mRNA levels were measured by real-time PCR. Data are expressed as  $2^{-\Delta Ct}$ . **(D)** In vitro 3D epidermal model was incubated for 24 h with increasing paclitaxel concentrations. VEGF protein levels were analyzed by Western blotting. Quantification was performed by densitometry and normalized to  $\beta$ -actin. Results are expressed as mean  $\pm$  standard deviation of three independent experiments ( $n = 3$ ). Multiple comparisons analysis of variance (ANOVA) was followed by the post hoc Bonferroni test. \*  $p < 0.05$  vs. control. PTX: paclitaxel.

## 5. NF- $\kappa$ B Transcription Factor Activation by Paclitaxel

The effect of paclitaxel on NF- $\kappa$ B activation was evaluated in the 3D epidermis model. The 3D model was incubated for 1 h with paclitaxel and both NF- $\kappa$ B unphosphorylated (**Figure 6A**) and phosphorylated (**Figure 6B**) forms were analyzed by Western blot. While the unphosphorylated form of the protein remained stable after incubation with all paclitaxel concentrations, NF- $\kappa$ B phosphorylation increased at all doses.

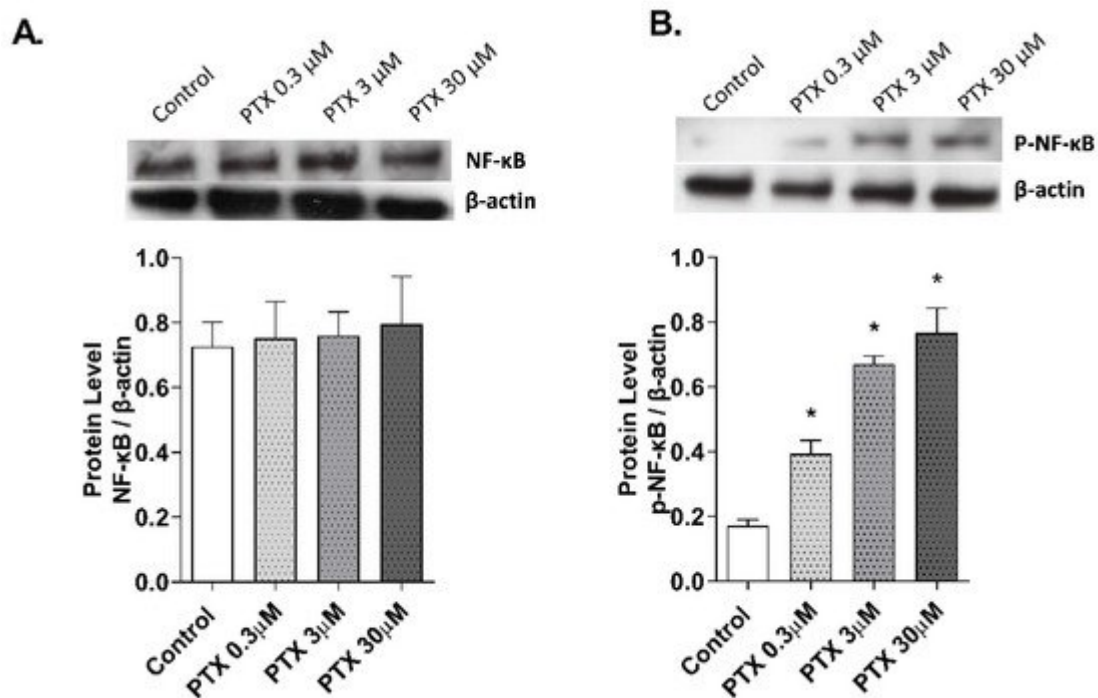


**Figure 6.** Paclitaxel activates the transcription factor NF- $\kappa$ B in a 3D epidermal model. The 3D epidermis was incubated for 1 h with increasing paclitaxel concentrations. **(A)** NF- $\kappa$ B and **(B)** p-NF- $\kappa$ B protein levels were analyzed by Western blotting. Quantification was performed by densitometry and normalized to  $\beta$ -actin. Results are

expressed as mean  $\pm$  standard deviation of three independent experiments ( $n = 3$ ). Multiple comparisons analysis of variance (ANOVA) was followed by the post hoc Bonferroni test. \*  $p < 0.05$  vs. control. PTX: paclitaxel.

## 6. TLR4 Mediates Paclitaxel Effects on Human Keratinocytes

Paclitaxel is a ligand to TLR4, which is expressed on innate immune cells, including macrophages [13][14]. However, there is no evidence in human skin. In this work, NHEK cells were transiently transfected with siRNA (-) control and siRNA-TLR4 to reduce TLR4 expression. The stimulation of NHEK cells with paclitaxel 3  $\mu$ M on pro-inflammatory IL-1 $\alpha$ , IL-6, and IL-8 cytokine release, and ROS production including SOD1, NOX4, and Nrf2 was significantly inhibited in cells transfected with siRNA-TLR4 (Figure 7A–G). The effects of paclitaxel reducing the anti-apoptotic protein BCL2 were reduced in siRNA-TLR4 treated cells (Figure 7H). The siRNA-TLR4 transfection also abrogated the effects of paclitaxel on eNOS and VEGF expression (Figure 7I,J) and reduced the phosphorylation of NF- $\kappa$ B in NHEK cells (Figure 7K).

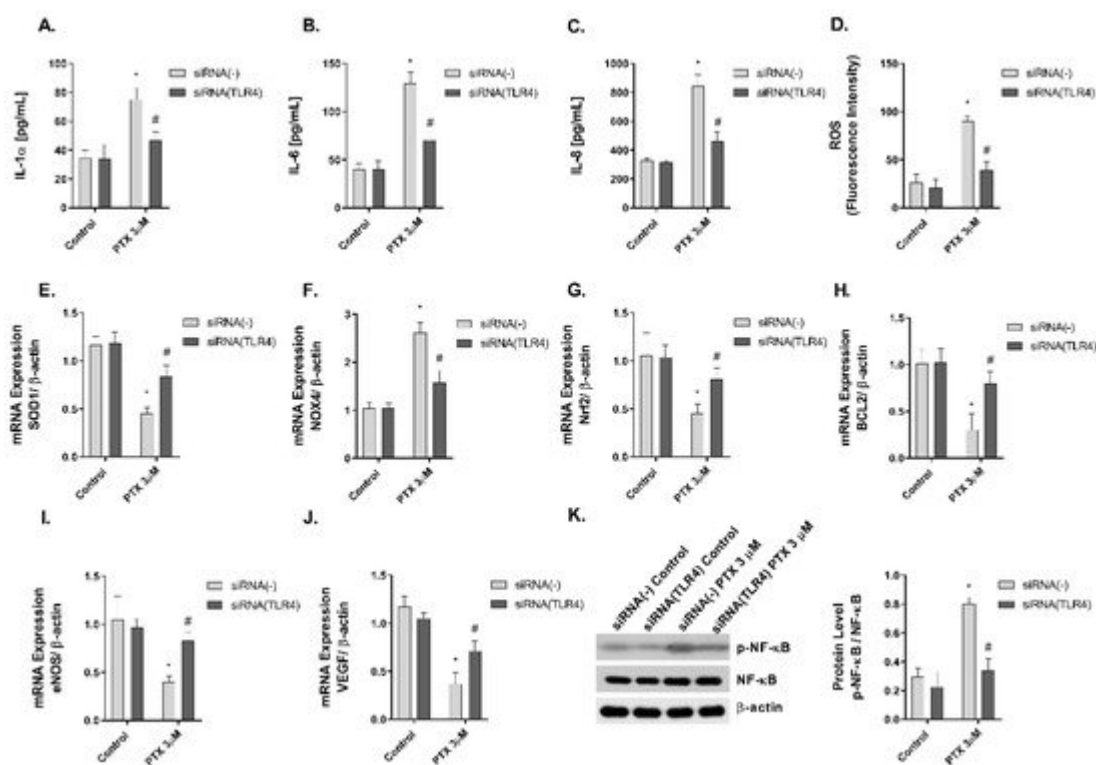


**Figure 7.** The effect of paclitaxel modulating inflammation, oxidative stress, apoptosis angiogenesis, and p-NF- $\kappa$ B is reduced in siRNA-TLR4 transiently transfected keratinocytes. Normal human epidermal keratinocytes (NHEK) were transiently transfected with control siRNA (-) or siRNA-TLR-4 and incubated for 24 h with paclitaxel 3  $\mu$ M. (A–C) IL-1 $\alpha$ , IL-6 and IL-8 supernatant levels were measured by ELISA. (D) Reactive oxygen species (ROS) were measured using H<sub>2</sub>DCF-DA assay in NHEK stimulated with paclitaxel for 4 h. (E–J) The expression of SOD1, NOX4, Nrf2, BCL2, eNOS, and VEGF was measured by real-time PCR. Data are expressed as  $2^{-\Delta\Delta Ct}$ . (K) NHEK cells were incubated for 1 h with paclitaxel concentrations. NF- $\kappa$ B and p-NF- $\kappa$ B protein levels were analyzed by Western blotting. Quantification was performed by densitometry and normalized to NF- $\kappa$ B/ $\beta$ -actin. Results are expressed as mean  $\pm$  standard deviation of three independent experiments ( $n = 3$ ). Multiple comparisons analysis

of variance (ANOVA) was followed by the post hoc Bonferroni test. \*  $p < 0.05$  vs. siRNA (-) Control. #  $p < 0.05$  vs. siRNA (-) PTX 3  $\mu\text{M}$ . PTX: paclitaxel.

## 7. Researches and Findings

Paclitaxel accumulates in endothelial cells [15] and exhibits a strong anti-angiogenic activity in cancer cells through the suppression of VEGF expression [10][11]. VEGF takes part in the angiogenesis signaling pathway by activating the endothelial nitric oxide synthase eNOS [16], which has reduced expression after paclitaxel treatment in endothelial cells [12][17]. Physiological levels of nitric oxide (NO) are required to maintain the normal functioning of cells, including keratinocytes. NO is vital as a signaling molecule regulating multiple epidermal functions, including keratinocyte proliferation and differentiation, apoptosis, migration, and oxidative stress, as well as cytokine production [18]. NO is produced by eNOS, that is expressed in human keratinocytes in a similar way that VEGF [18][19].

After paclitaxel treatment, activation of NF- $\kappa$ B transcription factor has been shown to play an important role in the regulation of inflammation, apoptosis, and cell cycle progression [20]. This transcription factor has also been associated with paclitaxel-induced ROS production and angiogenesis [9]. Between the different activators of NF- $\kappa$ B, TLR4 plays an important role in the innate immune response. The activation of TLR4 triggers different molecular pathways including JNK, P38 and NF- $\kappa$ B [21]. Previous reports have shown that paclitaxel can activate TLR4 in macrophages and dendritic cells, mimicking the effects of lipopolysaccharide secreting inflammatory cytokines [13][22]. TLR4 is expressed in human keratinocytes and its activation has been related to inflammatory, oxidative, and anti-proliferative effects [23], showing antineoplastic effects in cutaneous squamous cell carcinoma [24]. The reduction of TLR4 expression by siRNA-TLR4 partially abrogated the cellular effects induced by paclitaxel in keratinocytes. Currently, the dermatological adverse effects of paclitaxel have been described from a clinical perspective, but the knowledge about their cellular and molecular mechanisms is lagging. There is limited literature in which the effects of paclitaxel in healthy keratinocytes are explained. However, our results present novel evidence of the effects of paclitaxel on skin. Paclitaxel activates TLR-4 and promotes NF- $\kappa$ B phosphorylation, which results in the increase of oxidative stress, inflammation, and apoptosis, and the reduction of angiogenesis. These events could explain the direct skin side effects of paclitaxel in healthy skin, although the interplay between the different cellular processes and the associated signaling pathways are yet to be discovered.

## References

1. Perkins, M.A.; Osterhues, M.A.; Farage, M.A.; Robinson, M.K. A noninvasive method to assess skin irritation and compromised skin conditions using simple tape adsorption of molecular markers of inflammation. *Skin Res. Technol.* 2001, 7, 227–237.
2. Jensen, L.E. Targeting the IL-1 family members in skin inflammation. *Curr. Opin. Investig. Drugs* 2010, 11, 1211–1220.

3. Gröne, A. Keratinocytes and cytokines. *Vet. Immunol. Immunopathol.* 2002, 88, 1–12.
4. Wang, T.-H.; Chan, Y.-H.; Chen, C.-W.; Kung, W.-H.; Lee, Y.-S.; Wang, S.-T.; Chang, T.-C.; Wang, H.-S. Paclitaxel (Taxol) upregulates expression of functional interleukin-6 in human ovarian cancer cells through multiple signaling pathways. *Oncogene* 2006, 25, 4857–4866.
5. Lee, L.F.; Li, G.; Templeton, D.J.; Ting, J.P. Paclitaxel (Taxol)-induced gene expression and cell death are both mediated by the activation of c-Jun NH2-terminal kinase (JNK/SAPK). *J. Biol. Chem.* 1998, 273, 28253–28260.
6. Collins, T.S.; Lee, L.F.; Ting, J.P. Paclitaxel up-regulates interleukin-8 synthesis in human lung carcinoma through an NF-kappaB- and AP-1-dependent mechanism. *Cancer Immunol. Immunother.* 2000, 49, 78–84.
7. Lisse, T.S.; Middleton, L.J.; Pellegrini, A.D.; Martin, P.B.; Spaulding, E.L.; Lopes, O.; Brochu, E.A.; Carter, E.V.; Waldron, A.; Rieger, S. Paclitaxel-induced epithelial damage and ectopic MMP-13 expression promotes neurotoxicity in zebrafish. *Proc. Natl. Acad. Sci. USA* 2016, 113, E2189–E2198.
8. Alexandre, J.; Hu, Y.; Lu, W.; Pelicano, H.; Huang, P. Novel action of paclitaxel against cancer cells: Bystander effect mediated by reactive oxygen species. *Cancer Res.* 2007, 67, 3512–3517.
9. Kim, H.S.; Oh, J.M.; Jin, D.H.; Yang, K.-H.; Moon, E.-Y. Paclitaxel induces vascular endothelial growth factor expression through reactive oxygen species production. *Pharmacology* 2008, 81, 317–324.
10. Belotti, D.; Vergani, V.; Drudis, T.; Borsotti, P.; Pitelli, M.R.; Viale, G.; Giavazzi, R.; Taraboletti, G. The microtubule-affecting drug paclitaxel has antiangiogenic activity. *Clin. Cancer Res.* 1996, 2, 1843–1849.
11. Ai, B.; Bie, Z.; Zhang, S.; Li, A. Paclitaxel targets VEGF-mediated angiogenesis in ovarian cancer treatment. *Am. J. Cancer Res.* 2016, 6, 1624–1635.
12. Mikula-Pietrasik, J.; Witucka, A.; Pakula, M.; Uruski, P.; Begier-Krasińska, B.; Niklas, A.; Tykarski, A.; Książek, K. Comprehensive review on how platinum- and taxane-based chemotherapy of ovarian cancer affects biology of normal cells. *Cell. Mol. Life Sci.* 2019, 76, 681–697.
13. Byrd-Leifer, C.A.; Block, E.F.; Takeda, K.; Akira, S.; Ding, A. The role of MyD88 and TLR4 in the LPS-mimetic activity of Taxol. *Eur. J. Immunol.* 2001, 31, 2448–2457.
14. Wang, A.C.; Su, Q.B.; Wu, F.X.; Zhang, X.L.; Liu, P.S. Role of TLR4 for paclitaxel chemotherapy in human epithelial ovarian cancer cells. *Eur. J. Clin. Investig.* 2009, 39, 157–164.
15. Merchan, J.R.; Jayaram, D.R.; Supko, J.G.; He, X.; Buble, G.J.; Sukhatme, V.P. Increased endothelial uptake of paclitaxel as a potential mechanism for its antiangiogenic effects: Potentiation by Cox-2 inhibition. *Int. J. Cancer* 2005, 113, 490–498.

16. Cai, J.; Jiang, W.G.; Ahmed, A.; Boulton, M. Vascular endothelial growth factor-induced endothelial cell proliferation is regulated by interaction between VEGFR-2, SH-PTP1 and eNOS. *Microvasc. Res.* 2006, 71, 20–31.
17. Hayashi, S.; Yamamoto, A.; You, F.; Yamashita, K.; Ikegame, Y.; Tawada, M.; Yoshimori, T.; Shimizu, S.; Nakashima, S. The Stent-Eluting Drugs Sirolimus and Paclitaxel Suppress Healing of the Endothelium by Induction of Autophagy. *Am. J. Pathol.* 2009, 175, 2226–2234.
18. Man, M.-Q.; Wakefield, J.S.; Mauro, T.M.; Elias, P.M. Role of nitric oxide in regulating epidermal permeability barrier function. *Exp. Dermatol.* 2021.
19. Wang, Y.; Graves, D.T. Keratinocyte Function in Normal and Diabetic Wounds and Modulation by FOXO1. *J. Diabetes Res.* 2020, 2020, 3714704.
20. Hoesel, B.; Schmid, J.A. The complexity of NF- $\kappa$ B signaling in inflammation and cancer. *Mol. Cancer* 2013, 12, 86.
21. O'Neill, L.A.J.; Bowie, A.G. The family of five: TIR-domain-containing adaptors in Toll-like receptor signalling. *Nat. Rev. Immunol.* 2007, 7, 353–364.
22. Bracci, L.; Schiavoni, G.; Sistigu, A.; Belardelli, F. Immune-based mechanisms of cytotoxic chemotherapy: Implications for the design of novel and rationale-based combined treatments against cancer. *Cell Death Differ.* 2014, 21, 15–25.
23. Iotzova-Weiss, G.; Freiburger, S.N.; Johansen, P.; Kamarachev, J.; Guenova, E.; Dziunycz, P.J.; Roux, G.A.; Neu, J.; Hofbauer, G.F.L. TLR4 as a negative regulator of keratinocyte proliferation. *PLoS ONE* 2017, 12, e0185668.
24. Mikami, E.; Kudo, M.; Ohashi, R.; Kawahara, K.; Kawamoto, Y.; Teduka, K.; Fujii, T.; Kitamura, T.; Kure, S.; Ishino, K.; et al. Toll-like receptor 4 plays a tumor-suppressive role in cutaneous squamous cell carcinoma. *Int. J. Oncol.* 2019, 54, 2179–2188.

---

Retrieved from <https://encyclopedia.pub/entry/history/show/47850>